Supplementary information for

Stretchable and High-Performance Supercapacitors with Crumpled Graphene Papers

Jianfeng Zang[a,b,c], Changyong Cao[c]*, Yaying Feng[c]*, Jie Liu[d], Xuanhe Zhao[c,e,f, 1]*

[a] *School of Optical and Electronic Information, Huazhong University of Science and Technology, Wuhan, Hubei 430074, China;* [b] *Innovation Institute, Huazhong University of Science and Technology, Wuhan, Hubei, 430074, China;* [c] *Department of Mechanical Engineering and Materials Science, Duke University, Durham, NC 27708, USA;* [d] *Department of Chemistry, Duke University, Durham, NC 27708, USA;* [e] *Soft Active Materials Laboratory, Department of Mechanical Engineering, Massachusetts Institute of Technology, Cambridge, MA 02139, USA;* [f] *Department of Civil and Environmental Engineering, Massachusetts Institute of Technology, Cambridge, MA 02139, USA;*

[1] To whom correspondence should be addressed. Email: zhaox@mit.edu

* These authors contributed equally to this work.

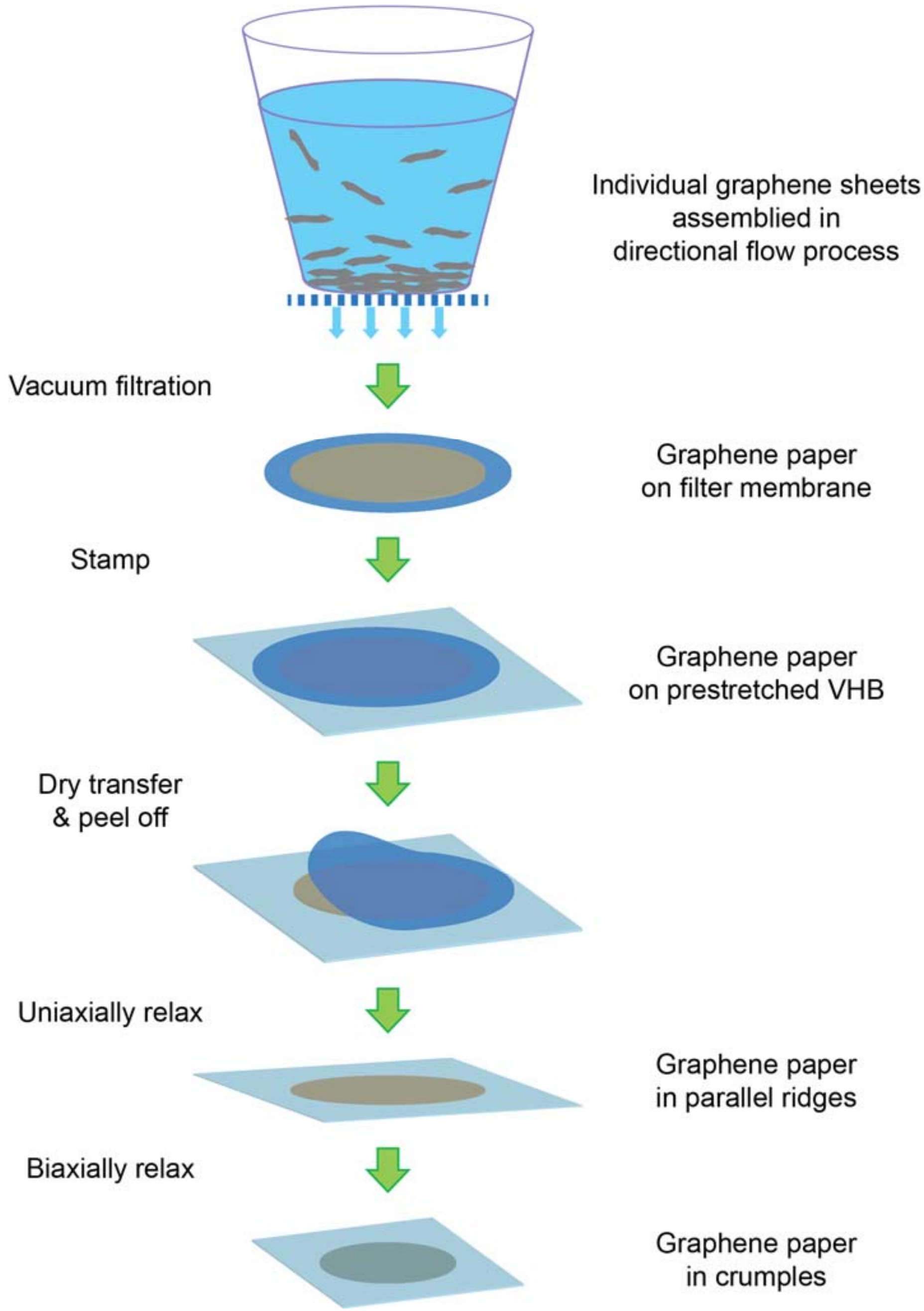

Fig. S1. Schematic illustration of the fabrication process of the crumpled graphene paper.

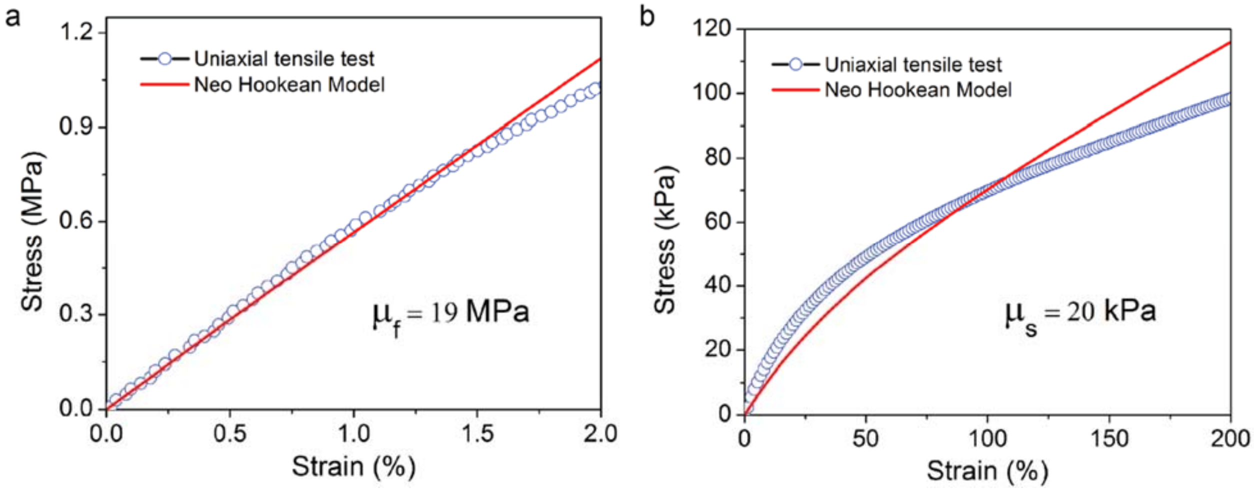

Fig. S2. Uniaxial tensile test of the graphene paper and VHB elastomer film. (**a**) Nominal stress vs. strain curve of the graphene paper under uniaxial tension. When the strain is less than 2%, graphene paper follows the neo-Hookean model with initial shear modulus $\mu_f = 19$ MPa. The thickness of the graphene paper is ~90 µm measured at hydrated state. (**b**) Nominal stress vs. strain curve of the VHB elastomer film under uniaxial tension. When the strain is less than 200%, the elastomer film approximates the neo-Hooke model with initial shear modulus $\mu_s = 20$ kPa.

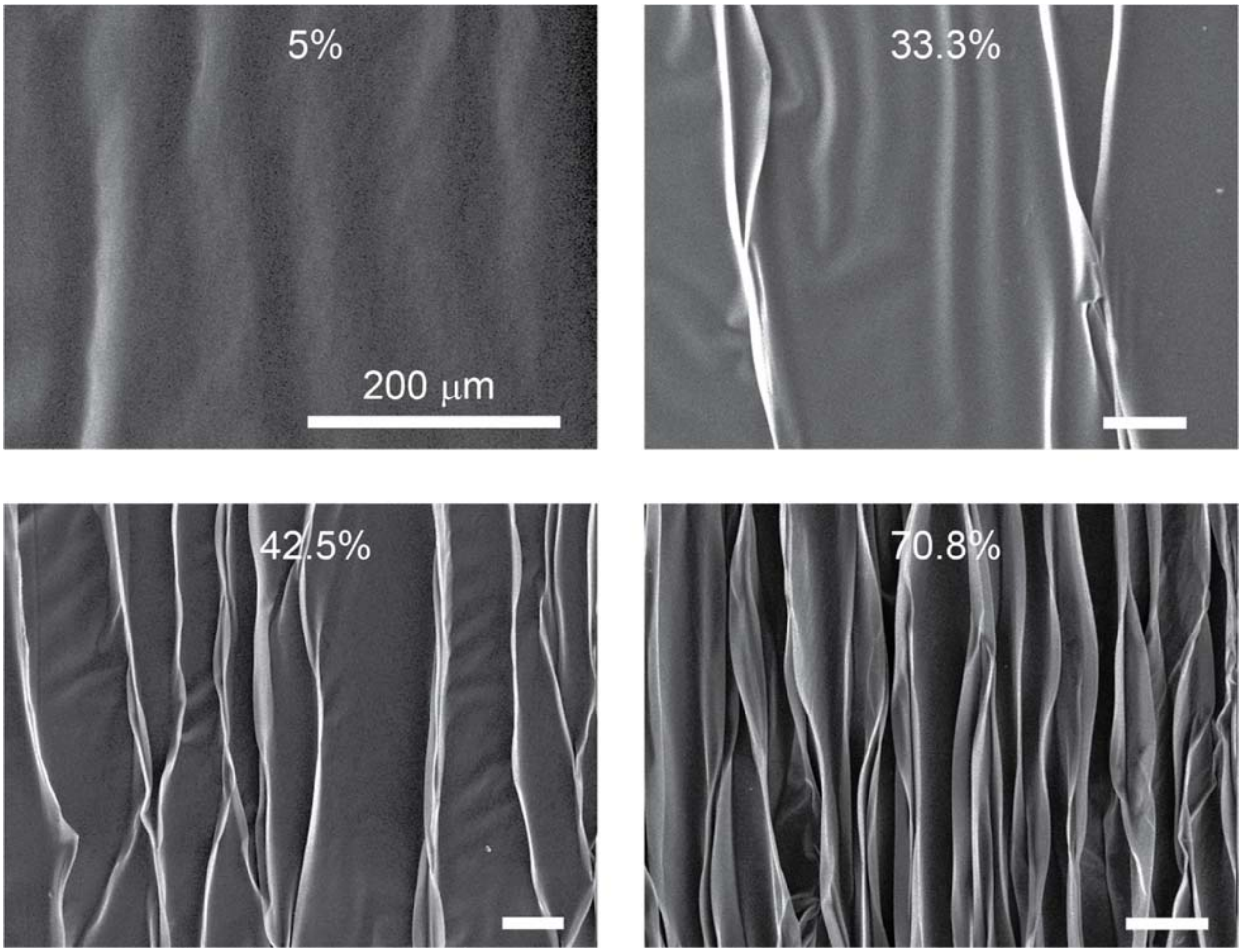

Fig. S3. Evolution of the instability patterns in a graphene paper (H_f =2 μm) on a uniaxially prestretched elastomeric film ($\varepsilon_{pre1} = 250\%, \varepsilon_{pre2} = 0\%$) relaxed uniaxially. The nominal compressive strains in the graphene paper are respectively 5%, 33.3%, 42.5%, and 70.8%. The graphene paper first forms wrinkles, which then evolve into localized ridges.

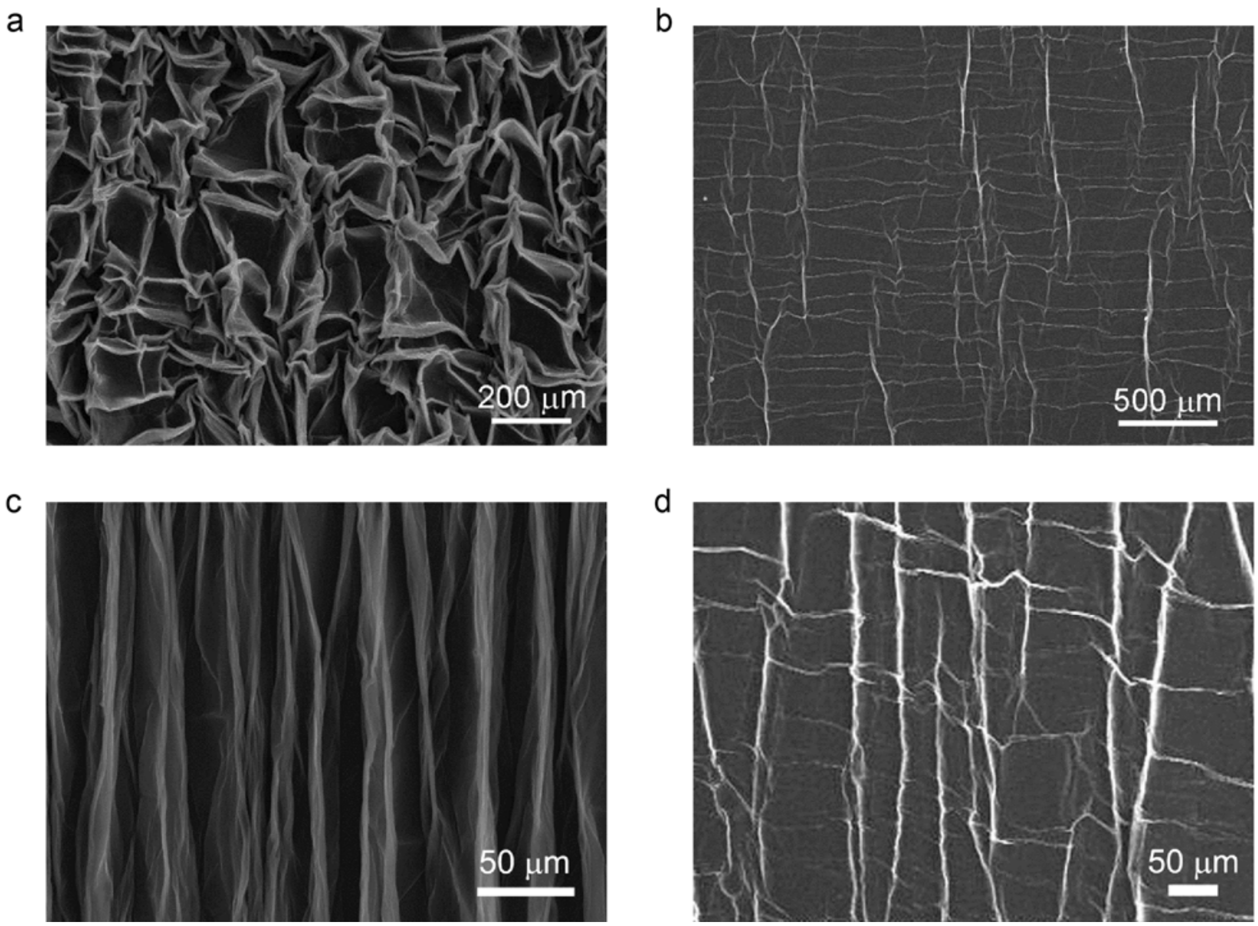

Fig. S4. SEM images of folding and unfolding processes of the crumpled graphene papers. (**a**) Folding of graphene paper on an elastomer film with biaxial pre-strains of 200%×200%. (**b**) Unfolding of the folded graphene paper in (**a**) by stretching the elastomer film to biaxial strain of 150%×150%. (**c**) Folding of graphene paper on an elastomer film with uniaxial pre-strains of 400%. (**d**) Unfolding of the folded graphene paper in (**c**) by stretching the elastomer film to uniaxial strain of 300%. The thickness of the graphene paper is ~2 μm measured at dehydrated state.

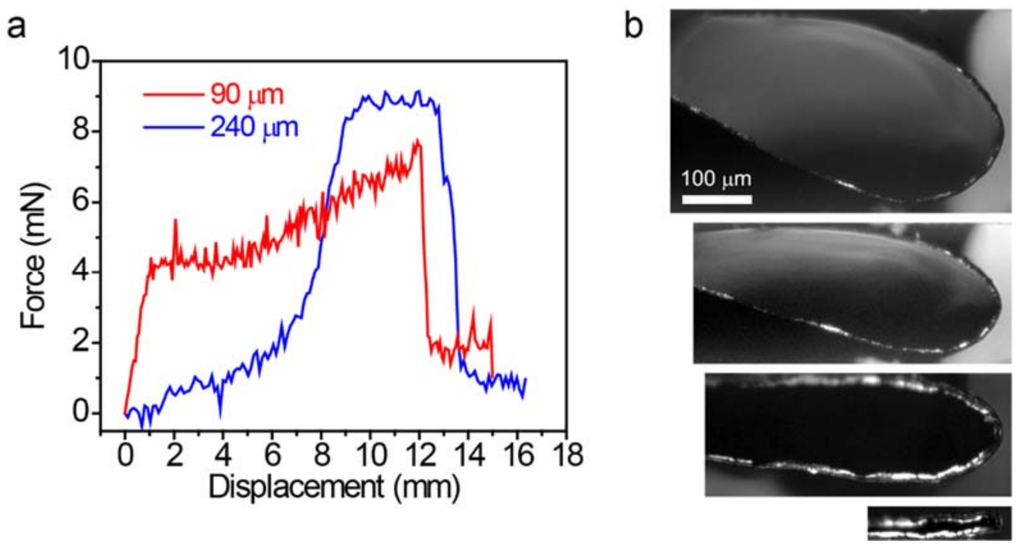

Fig. S5. Trouser and bending testing of graphene paper films. (**a**) Trouser test curves for two graphene paper hydrogel films with the thickness of 90 and 240 μm. According to the equation $G_C = 2F/h$, where G_C, F, and h are fracture energy, force, and thickness, the fracture energy derived from (**a**) are 119 J m^{-2} for the 90 μm sample and 73 J m^{-2} for the 240 μm sample. The thicknesses of these two graphene paper films correspond to 2 μm and 5 μm respectively in the dried state after dehydration. (**b**) Optical images of a process for bending a graphene paper hydrogel film. The graphene paper maintains its integrity when it is fully folded.

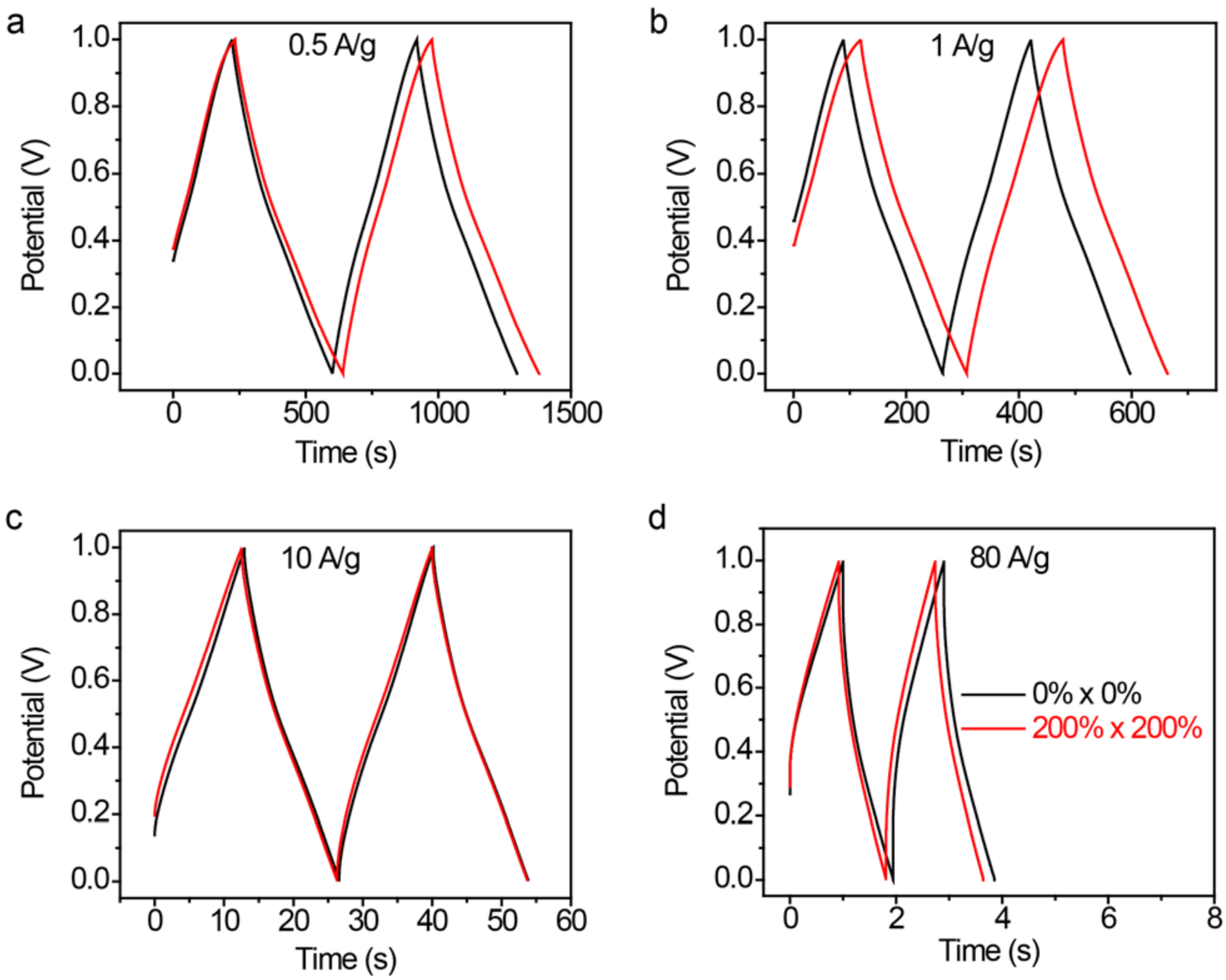

Fig. S6. The galvanostatic charge/discharge curves of the crumpled-graphene paper electrodes at the undeformed state and under a biaxial strain of 200%×200% at current densities of (**a**) 0.5, (**b**) 1, (**c**) 10, and (**d**) 80 A g^{-1}. The thickness of the graphene paper is ~2 µm measured at dehydrated state.

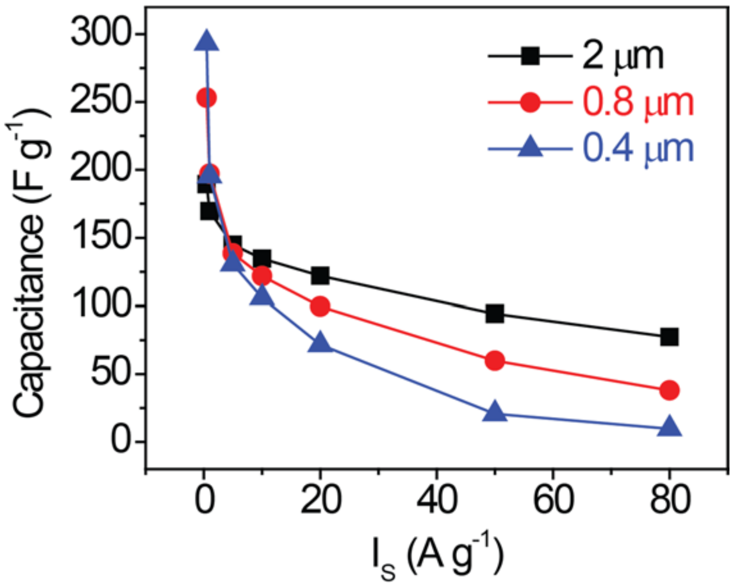

Fig. S7. Rate capability of crumpled-graphene papers with different thicknesses, 2 µm, 0.8 µm and 0.4 µm. Gravimetric capacitance measured at different charge/discharge current densities (I_s =0.5, 1.0, 5.0, 10, 20, 50, and 80 Ag^{-1}). The tests were carried out in 1.0 M H_2SO_4. The thicknesses of the graphene papers were measured at dehydrated state.

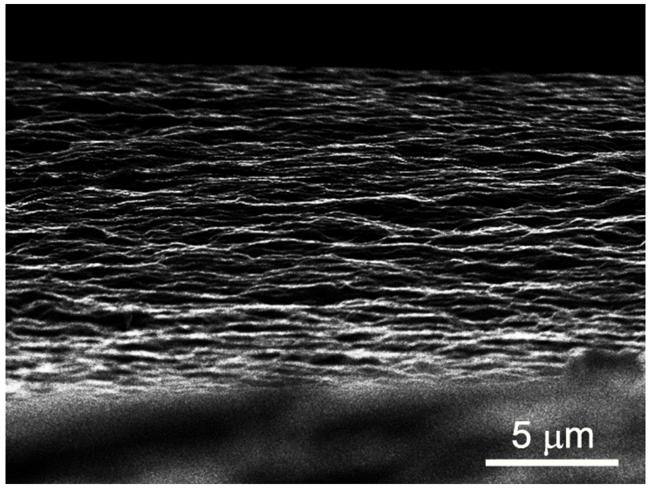

Fig. S8. SEM image of the cross section of a graphene paper showing its porous structure.

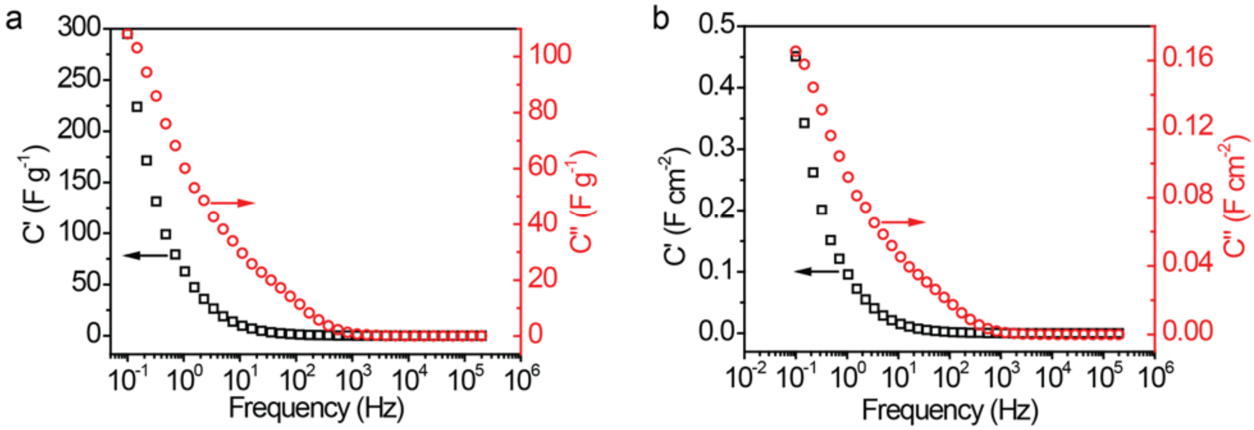

Fig. S9. Fequency dependent gravimetric (**a**) and areal capacitance (**b**) of the crumpled-graphene paper electrode for supercapacitor. The CG-paper was prepared by relaxing a biaxially pre-stretched elastomer film with $\varepsilon_{pre1} = \varepsilon_{pre2} = 400\%$. The thickness of the graphene paper is ~2 μm measured at dehydrated state.

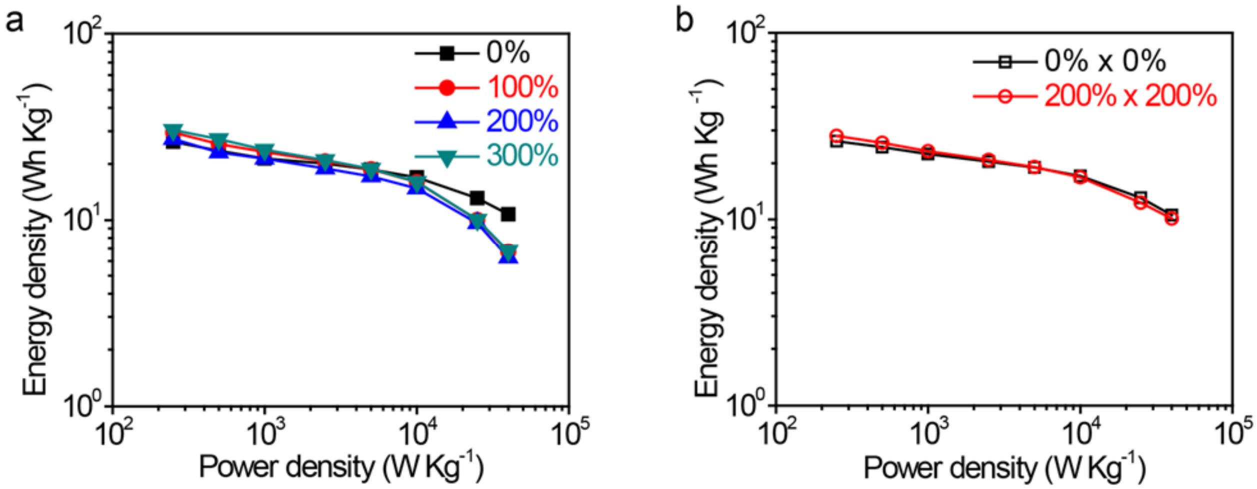

Fig. S10. Ragone plots of the crumpled-graphene paper electrodes under large deformations. Values were calculated by measuring the galvanostatic charge/discharge curves at current densities of 0.5, 1, 2, 5, 10, 20, 50, and 80 A g^{-1}. (**a**) Performance of the crumpled-graphene-paper electrodes under uniaxial strains of 0%, 100%, 200%, and 300%. (**b**) Performance of the crumpled-graphene-paper electrodes under biaxial strains of 0%×0% and 200%×200%. The thickness of the graphene paper is ~2 µm measured at dehydrated state.

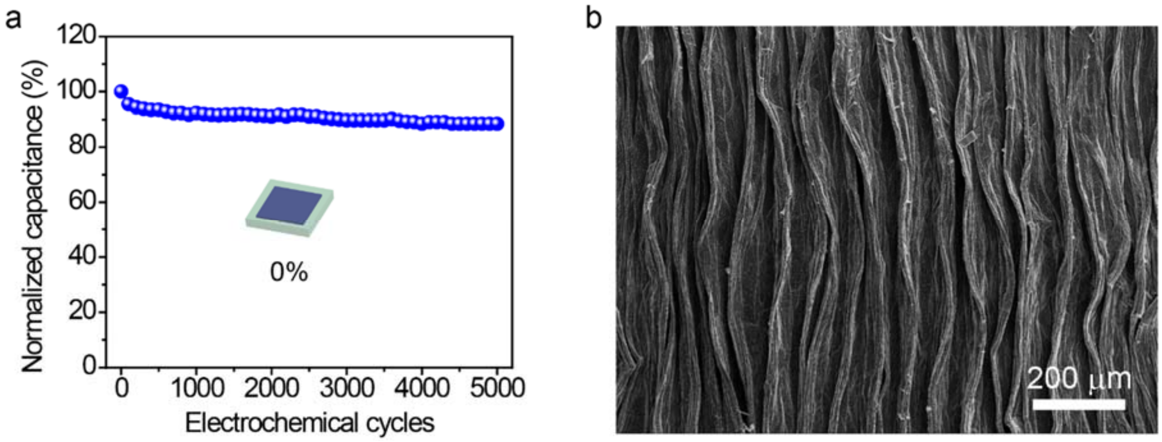

Fig. S11. Electrochemical cyclic stability of the CG-paper electrodes. (**a**) The normalized capacitance of the electrodes crumpled on uniaxially pre-stretched elastomer film with $\varepsilon_{pre1} = 400\%$ $\varepsilon_{pre2} = 50\%$, measured by 5000 galvanostatic charge/discharge cycles at 10 A g^{-1}. (**b**) SEM images of the CG-paper electrode after 5000 cycles. The thickness of the graphene paper is ~2 μm measured at dehydrated state.

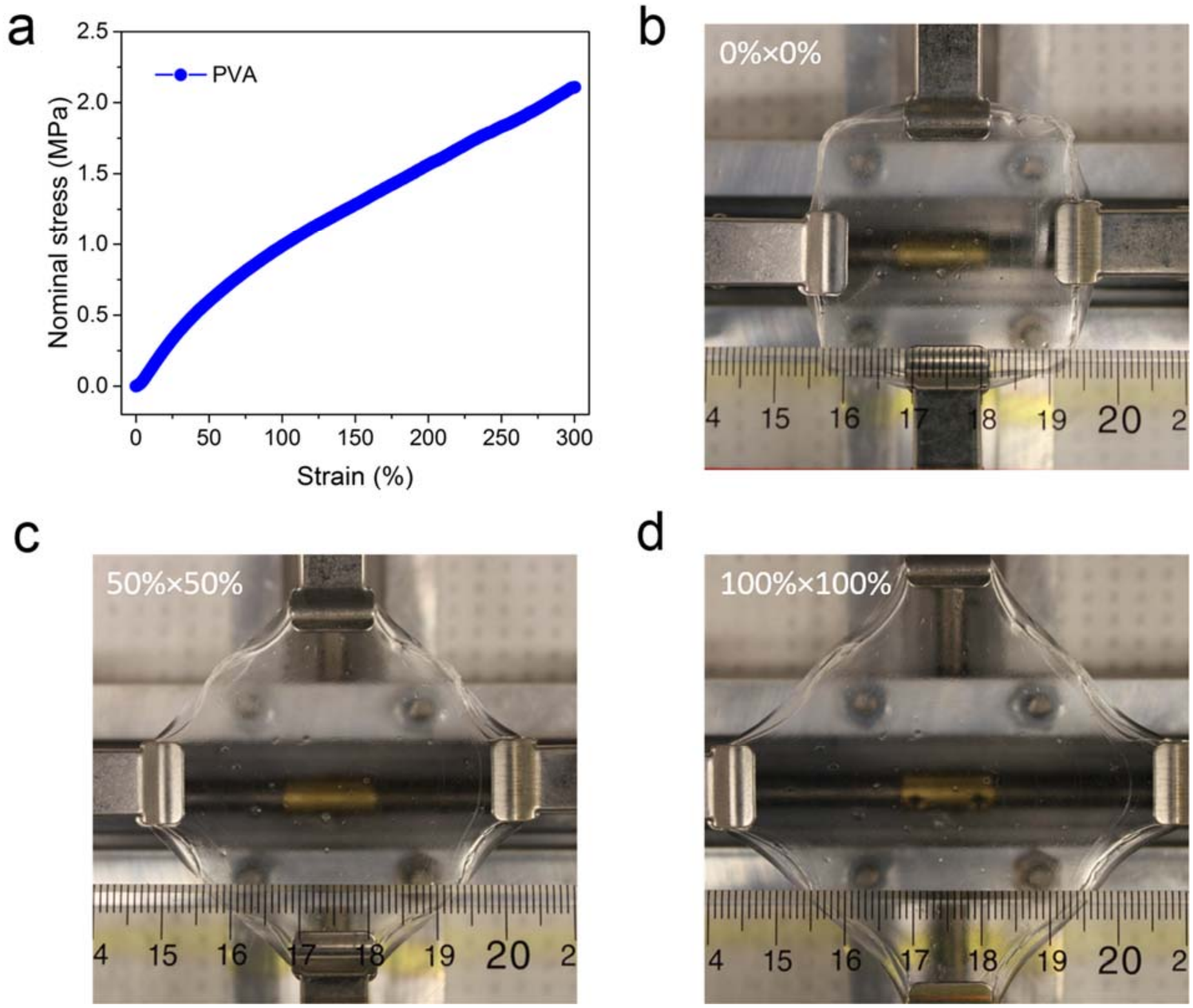

Fig. S12. Stretchability of PVA-H_3PO_4 film for the all-solid-state supercapcatiors. (**a**) The stress-strain curve obtained from the uniaxial tensile test in the strain range of 0% - 300%. Photos of a PVA-H_3PO_4 film biaxially stretched to different strains: (**b**) 0%×0%, (**c**) 50%×50% and (**d**) 100%×100%.

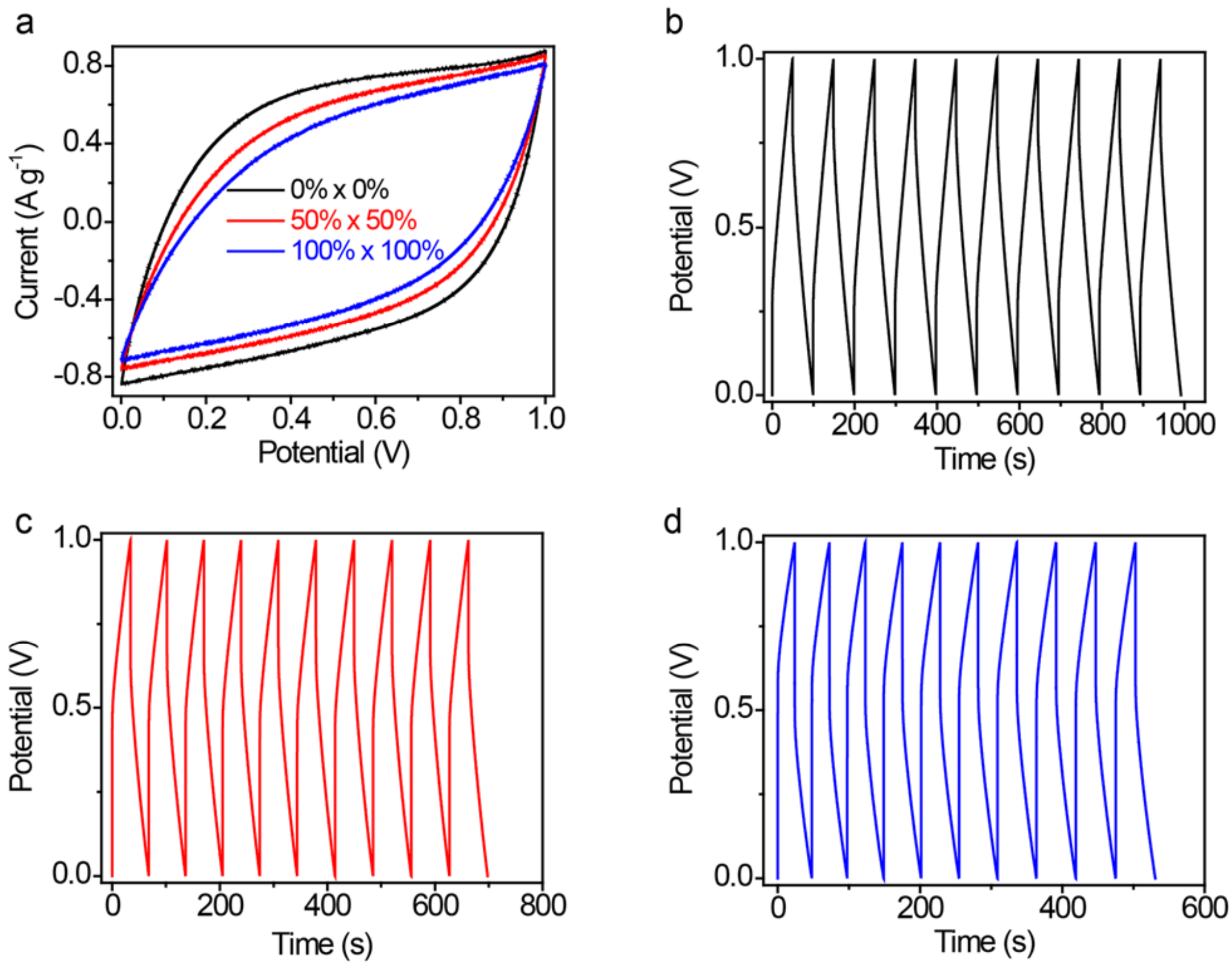

Fig. S13. Electrochemical performance of the stretchable supercapacitor under biaxial strains. (**a**) CV curves of the supercapacitor deformed by biaxial strains of 0%×0%, 50%×50% and 100%×100%, measured at a scan rate of 10 mV s^{-1}. Galvanostatic charge/discharge curves of the supercapacitor deformed by biaxial strains of (**b**) 0%×0%, (**c**) 50%×50%, and (**d**) 100%×100%, measured at a current density of 1 A g^{-1}. The thickness of the graphene paper is ~0.8 μm measured at dehydrated state.

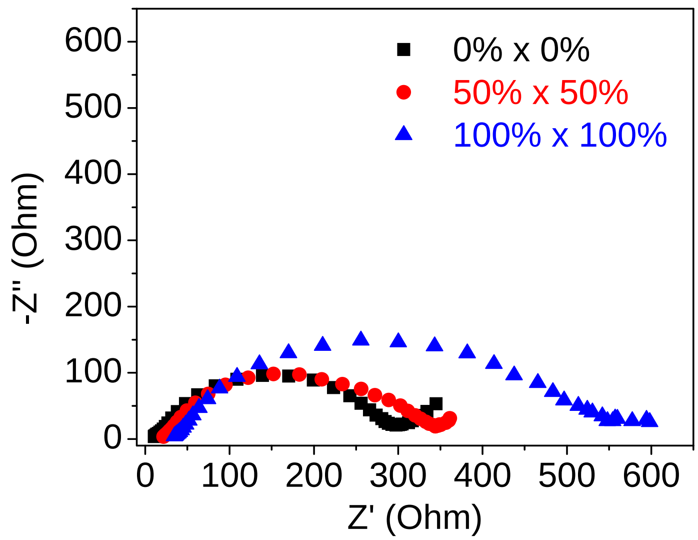

Fig. S14. Nyquist plots of the supercapacitor with biaxial strain of 0% × 0%, 50% × 50%, and 100% × 100%. The thickness of the graphene paper is ~0.8 μm measured at dehydrated state.

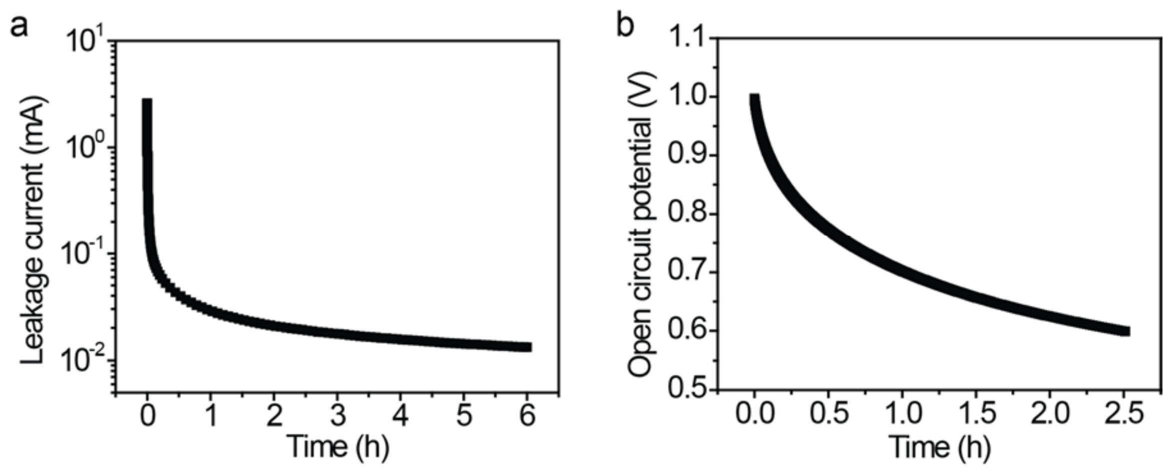

Fig. S15. Testing of self-discharge rate of a stretchable supercapacitor. (**a**) Leakage current measurement of a stretchable supercapacitor. A DC voltage of 1.0 V was applied across the capacitor; the current required to retain that voltage was measured over a period of 6 h. (**b**) Self-discharge curves of the supercapacitor obtained immediately after precharging. The open circuit potential across the supercapacitor are recorded over 60% the operation voltage of 1.0 V versus the course of time. The thickness of the graphene paper is ~0.8 μm measured at dehydrated state.